Consequences of Hydrophobic Mismatch between Lipids and Melibiose Permease on Melibiose Transport

Fabrice Dumas, Jean-François Tocanne, Gerard Leblanc,[‡] and Maria-Chantal Lebrun*

Institut de Pharmacologie et Biologie Structurale du CNRS,205, Route de Narbonne F-31077 Toulouse Cedex, France, Laboratoire de Physiologie des Membranes Cellulaires - LRC-CEA 16V, Université de Nice Sophia-Antipolis and CNRS (ERS 1253). 06238, Villefranche sur Mer Cedex, France

ABSTRACT: The structural and functional consequences of a mismatch between the hydrophobic thickness d_P of a transmembrane protein and that d_L of the supporting lipid bilayer were investigated using melibiose permease (MelB) from *Escherichia coli* reconstituted in a set of bis saturated and monounsaturated phosphatidylcholine species differing in acyl-chain length. Influence of MelB on the midpoint gel-to-liquid-phase transition temperature, T_m, of the saturated lipids was investigated through fluorescence polarization experiments, with 1,6-diphenyl-1,3,5-hexatriene as the probe, for varying protein/lipid molar ratio. Diagrams in temperature versus MelB concentration showed positive or negative shifts in T_m with the short-chain lipids DiC12:0-PC and DiC14:0-PC or the long-chain lipids DiC16:0-PC and DiC18:0-PC, respectively. Theoretical analysis of the data yielded a d_L value of 3.0 ± 0.1 nm for the protein, similar to the 3.02 nm estimated from hydropathy profiles. Influence of the acyl chain length on the carrier activity of MelB was investigated in the liquid phase, using the monounsaturated PCs. Binding of the sugar to the transporter showed no dependence on the acyl chain length. In contrast, counterflow and $\Delta\psi$-driven experiments revealed strong dependence of melibiose transport on the lipid acyl chain length. Similar bell-shaped transport versus acyl chain length profiles were obtained, optimal activity being supported by diC16:1-PC. On account of a d_P value of 2.65 nm for the lipid and of various local constraints which would all tend to elongate the acyl chains in contact with the protein, one can conclude that maximal activity was obtained when the hydrophobic thickness of the bilayer matched that of the protein.

The structure of biological membranes is governed mainly by complex interactions between lipids and integral membrane proteins, i.e., hydrophobic interactions between the acyl chains of the lipids and the membrane-spanning part of the proteins and polar interactions between the headgroups of the lipids and the amino acids of the hydrophilic domains of the proteins. Because any exposure to water of hydrophobic acyl chain segments or amino acid residues is energetically unfavorable, it has been suggested that optimal protein/lipid interactions require, in particular, good matching between the length of the membrane span of the proteins and the thickness of the hydrophobic core of the supporting lipid bilayer (1, 2). Computer simulations and experimental studies on peptides and proteins incorporated in lipid vesicles indicate that if the hydrophobic matching condition is not satisfied, the excess of energy which results may be relieved by changes in the lateral distribution of the lipid and protein partners or by changes in their conformation (see reviews in refs 3 and 4).

In terms of lateral distribution, protein aggregation has been predicted to occur (5, 6) and shown to take place for example in the case of the bacterial photosynthetic antenna protein (LHCP) (7), rhodopsin (8), and the (Ca²⁺, Mg²⁺)-ATPase (9). Hydrophobic mismatch may also trigger a

mechanism of protein/lipid molecular sorting, a theoretical concept (6) which has received experimental support with bacteriorhodopsin (10), the pulmonary surfactant protein SP-C (11), and lactose permease (12) reconstituted in binary lipid mixtures. In this respect, the hypothesis has been made that, along the protein synthetic pathway, the hydrophobic matching condition would play a significant role in the targeting and retention of membrane proteins in their respective compartments (endoplasmic reticulum, Golgi apparatus, and plasma membrane) (13−16).

In terms of conformation, proteins can affect the order of the acyl chains of the surrounding lipids (17) with consequences on their gel-fluid phase transition temperature (7, 18−21). Intrinsic membrane proteins exhibit a certain flexibility and hydrophobic mismatch may trigger conformational changes with consequences on their activity. Consistently, the (Ca²⁺, Mg²⁺)ATPase from rabbit muscle sarcoplasmic reticulum (9, 22−26) and the (Na⁺, K⁺)ATPase from porcine kidneys (27) reconstituted in monounsaturated PCs[1] of different chain lengths (diCn:1-PC) showed optimal activity at lipid chain length of around 18−20 carbon atoms, shorter or longer acyl chains supporting lower activity. Similarly, the activities of the human erythrocyte hexose transporter in diCn:1-PC (28), of the leucine transport system of *Lactococcus lactis* (29) and *Pseudomonas aeruginosa* (30) in PE/PC mixtures, of cytochrome *c* oxidase and the (F1,F0)-ATPase complex in diCn:1-PC (31) were also found to be

* To whom correspondence should be addressed. Phone: (33)-05 61 17 59 46. Fax: (33)-05 61 17 59 94. E-mail: chirio@ipbs.fr.
‡ Université de Nice Sophia-Antipolis and CNRS.

chain length dependent, with maximum activity around 16–18 carbon atoms. However, the question of whether a hydrophobic mismatch, specified quantitatively on the grounds of the hydrophobic thickness of the lipids and proteins, is responsible for the observed changes in protein activity remains to be elucidated.

In the present study, we examined the structural and functional consequences of hydrophobic mismatch using melibiose permease (MelB) reconstituted in a set of phosphatidylcholines differing in acyl chain length. Melibiose permease is a cation/sugar symporter from *Escherichia coli* which catalyzes cell accumulation of α-galactosides such as melibiose (*32–34*). MelB consists of 473 amino acids (M_r 53 kDa) (*35, 36*) and displays the characteristics of a polytopic protein with 12 α-helical transmembrane domains (*37–39*). A His-tagged protein has been overexpressed in *E. coli* and purified in active state to homogeneity and to amounts large enough to carry out biophysical studies (*36*). The extent of hydrophobic mismatch between MelB and the various lipid bilayers was determined by analyzing the influence of the protein on the phase transition temperature of the lipids. The influence of the lipid acyl chain length on the carrier activity was investigated in parallel. Through comparison of the hydrophobic length of the protein and the hydrophobic thickness of the various lipid bilayers, the data presented clearly show that the minimum lipid perturbation and the highest protein activity are found when the hydrophobic matching condition is optimum.

MATERIALS AND METHODS

Chemicals. [³H]Melibiose and dansyl galactoside (Dns²-S-Gal) were synthesized under the direction of Dr. B. Rousseau (Service des Molécules Marquées, Commissariat à l'Energie Atomique, France). Purity of Dns²-S-Gal was checked by mass spectrometry and NMR analysis. [³H]Tetraphenylphosphonium-bromide was purchased from Amersham Corp., and tetraphenylphosphonium-bromide (TPP) from Fluka. The Ni-NTA resin was obtained from Qiagen, Inc. Anion-exchange resin (Macro-Prep Q support) and Bio-Beads SM-2 were obtained from Bio-Rad Lab., Inc. Dilauroylphosphatidylcholine (diC12:0-PC), dimyristoylphosphatidylcholine (diC14:0-PC), dipalmitoylphosphatidylcholine (diC16:0-PC), distearoylphosphatidylcholine (diC18:0-PC), dimyristoleoylphosphatidylcholine (diC14:1-PC), dipalmitoleoylphosphatidylcholine (diC16:1-PC), and dioleoylphosphatidylcholine (diC18:1-PC) were purchased from Sigma Chemical Co. (St. Louis). Stock solutions of valinomycin (Sigma), monensine (Sigma), and carbonyl-cyanide-*p*-trichlorophenylhydrazone (CCCP) (Boehringer.Manheim) were prepared in DMSO and ethanol, respectively.

Bacterial Strains and Plasmids. E. coli DW2–R (*40*), a *rec*A⁻ derivative of strain DW2 (Δ*mel*, Δ*lacZY*) (*41*) was

transformed with a plasmid expressing wild-type His-tagged-MelB (pK31ΔAHB) (*42*). Transformed DW2–R cells were grown to OD600 = 2 at 30 °C in 200 L of culture at the Centre de Fermentation (CNRS Marseille, France) as described (*42*).

Melibiose Permease Purification. All steps were performed at 0–4 °C as described by Pourcher et al. (*36*). Briefly, inverted membrane vesicles (IMVs) were prepared using a French press (American Instrument Co., pressure, 18 000 psi) and cells resuspended in a medium containing 50 mM NaH₂PO₄ (pH 8), 10 mM Tris-HCl (pH 8), 0.6 M NaCl, 20% glycerol, 5 mM β-mercaptoethanol, and 10 mM imidazole. IMVs (~15 mg/mL) were solubilized for 20 min in the presence of 3% dodecylmaltoside and the sample was centrifuged (280000*g*, 30 min). MelB was purified from the supernatant using Ni-NTA chromatography followed by Mono-Q chromatography. At this stage, determination of the protein and phosphorus content showed that one molecule of melibiose permease remained associated with approximatively six to eight molecules of the native bacterial phospholipids. The purified melibiose permease was then concentrated by means of a Centricon apparatus (Millipore) to 1 mg of protein/mL and immediately submitted to the reconstitution procedure.

Reconstitution of Melibiose Permease in Lipid Vesicles. This was carried out using a procedure involving detergent adsorption on polystyrene beads (*43–45*). Liposomes were prepared using the reversed-phase method (*46*). Fractions of purified MelB (1 mg of protein/mL) in the detergent were mixed with given amounts of the liposome preparations to the desired protein-to-lipid ratio. SM₂-Biobeads were added to the lipid/detergent/protein mixture (750 mg of Biobeads for 1 mL dispersion), and the samples were incubated overnight under gentle stirring. Each proteoliposome preparation so obtained was submitted to a 5–40% sucrose density gradient as described by Heyn and Dencher (*47*). The proteoliposome band was collected, washed by dialysis (48 h), and submitted to repeated freezing-thawing-sonication-wash cycles in Na⁺-free, 10 mM KH₂PO₄ (pH 7.0) buffer, to eliminate sucrose and NaCl from the inner compartment of the vesicle. Proteoliposome suspensions were analyzed with respect to their protein and lipid content. To check whether this reconstitution technique yielded unilamellar vesicles, the following procedure was applied. Reconstitutions were carried out with lipid samples containing 1 mol % of the fluorescent lipid probe N-NBD-PE, and fluorescence was measured in the presence of an increasing concentration of cobalt ions in the proteoliposome suspensions. Fluorescence quenching stabilized at 50% for CoCl₂ concentrations of 100 μM and above and at 100% upon further addition of the detergent dodecylmaltoside (0.1%) to the suspension, thus indicating the presence of unilamellar lipid vesicles.

Melibiose Transport and Counterflow Experiments. All experiments were carried out at 20 °C. Δψ-Driven melibiose uptake was performed as follows: proteoliposomes (1.5 mg of protein/mL) were incubated for 5 min in 100 mM KH₂PO₄ (pH 7.0) buffer and 0.2 μM valinomycin. Aliquots of the proteoliposome suspension were subsequently diluted 10-fold in a 100 mM NaH₂PO₄ (pH 7.0) buffer supplemented with 0.2 μM valinomycin and 400 μM [³H]melibiose (8 mCi/mmol). At given intervals of time, aliquots (1 mL) of the

---

[1] Abbreviations: PC, phosphatidylcholine; diC*n*:0-PC and diC*n*:1-PC, bis saturated and monounsaturated phosphatidylcholines, *n* being the number of carbon atoms in the acyl chains; NBD, 7-nitrobenz-2-oxa-1,3-diazol-4-yl; N-NBD-PE, *N*-(7-nitro-2,1,3-benzoxadiazol-4-yl)-phosphatidylethanolamine; DPH, 1,6-diphenyl-1,3,5-hexatriene; MelB, melibiose permease; melibiose, 6-*O*-α-D-galactopyranosyl-D-glucose; Dns²-S-Gal, 2′-(*N*-dansyl)aminoethyl-1-thio-β-D-galactopyranoside; Trp, tryptophan; His, histidine; FRET, fluorescence resonance energy transfer; TPP, tetraphenylphosphonium-bromide; Δψ, the electrical potential across the membrane.

diluted suspension were filtered on a 0.2 μm glass-fiber filter (Whatman, GF/B Prolabo) and the filter was washed twice with 5 mL of ice-cold NaH_2PO_4 (pH 7.0) buffer. Radioactivity associated with the proteoliposomes adsorbed on the filter was determined by liquid scintillation spectrophotometry. Stock solutions of uncoupler (prepared in 25% ethanol), when added to the transport incubation medium, were diluted 400-fold. The rate of melibiose transport (V_{max}) was determined from linear regression analysis of the kinetics data obtained within the first minute.

Counterflow experiments were performed as described (*48*). Proteoliposomes (1.5 mg of protein/mL), in a 100 mM KH_2PO_4, 10 mM NaH_2PO_4 (pH 7.0) buffer supplemented with 20 mM melibiose, were submitted to three freezing−thawing−sonication cycles for complete homogenization of the mixture between the inner and outer proteoliposome compartments. The suspension was then incubated overnight at 4 °C. CCCP (10 μM) and 0.75 μM monensine were added. Aliquots (10 μL) of the loaded proteoliposomes were then diluted into 150 μL of a 100 mM KH_2PO_4, 10 mM NaH_2-PO_4 (pH 7.0) buffer containing 3.2 nmol of [^{3}H]melibiose (3.2 Ci/mmol). At intervals of time, 10 μL of the suspension was filtered and washed as described above. Rates of melibiose transport were determined by linear regression analysis of the kinetics data obtained within the first minute.

Measurement of the Transmembrane Potential $\Delta\psi$. The electrical potential across the membrane ($\Delta\psi$, interior negative) was determined from the in/out distribution of a tritiated derivative of the lipophilic cation tetraphenylphosphonium (*29*). As described above for transport activity measurements, proteoliposomes were incubated 5 min in the presence of 100 mM KH_2PO_4, (pH 7.0) buffer and 0.2 μM valinomycin. Aliquots of a concentrated proteoliposome suspension (1.5 mg of protein/mL) were subsequently diluted 10-fold into a 100 mM NaH_2PO_4 (pH 7.0) buffer supplemented with 0.2 μM valinomycin. [^{3}H]Tetraphenylphosphonium-bromide (TPP, 2 μM) was then added. The amount of TPP accumulated in the proteoliposomes was evaluated using the filtration and radioactivity counting method described above for the transport measurements. $\Delta\psi$ was calculated according to the Nernst−Planck equation. The internal volume of the proteoliposomes was estimated from the amount of entrapped calcein as described (*49*).

Ligand Binding Measurements. Experiments were carried out with the fluorescent galactoside Dns^2-S-Gal, a high-affinity ligand of MelB (*42*). Binding of Dns^2-S-Gal to MelB was determined by measuring the fluorescence resonance energy transfer (FRET), which takes place between the Trp residues of the protein as the donors and the dansyl group of Dns^2-S-Gal as the acceptor (*42*). Proteoliposomes were resuspended at a concentration of 2.5 μg of protein/mL in 100 mM KH_2PO_4 (pH 7.0) buffer supplemented with 10 mM NaCl. The excitation wavelength was 295 nm, and fluorescence was recorded over the wavelength range 310−610 nm. The extent of FRET ($\Delta F = F_0 - F$) was determined from the fluorescence signal of the Trp residues in the absence (F_0) and in the presence (F) of an increasing concentration of Dns^2-S-Gal. F_0 and F were calculated by integrating the Trp emission spectra between 310 and 400 nm.

Fluorescence Polarization Measurements. Experiments were carried out using a T-format automatic apparatus of

our fabrication which has been described elsewhere (*21*). 1,6-Diphenyl-1,3,5-hexatriene (DPH) was used as the probe. The excitation wavelength was 360 nm, and fluorescence was measured over the wavelength range 400−500 nm. The polarization p is expressed as $p = (I_{\parallel} - I_{\perp})/(I_{\parallel} + I_{\perp})$.

Fluorescence Spectroscopy. Steady-state fluorescence measurements were performed at 20 °C with a 500 SLM-Aminco spectrofluorimeter equipped with 1 cm path-length cuvettes. In the wavelength range of interest (300−600 nm), absorbance of proteoliposomes dispersions was less than 0.1, thus enabling inner filter effects to be ignored. Absorption spectra were recorded with a Perkin-Elmer Lambda 5 UV−vis spectrophotometer.

Miscellaneous. Protein concentration was assayed by the method of Lowry in the presence of 0.5% (wt/vol) sodium dodecyl sulfate (*50*). Bovine serum albumin was used as a standard. Phospholipid concentration was assayed by measuring the phosphorus content (*51*).

RESULTS

Influence of Melibiose Permease on the Gel-to-Liquid-Phase Transition Temperature of Lipids. Purified MelB was reconstituted in diC12:0-PC, diC14:0-PC, diC16:0-PC, and diC18:0-PC at varying protein/lipid ratios, not exceeding 1/400. The midpoint transition temperature (T_m) of the lipids was determined through fluorescence polarization experiments and using DPH as the probe. Typical fluorescence polarization versus temperature curves are shown in Figure 1. On these curves, T_m was defined as the temperature corresponding to the inflection point and was measured using the double-tangent method. As can be seen, addition of MelB to the lipids brought about an upward or a downward shift in T_m, depending on the chain length of the lipids. The absence of significant effect of residual detergent molecules and/or endogenous phopholipids copurified with MelB on the T_m of the host lipids was assessed in the following way. First vesicles of diC12:0-PC, diC14:0-PC, diC16:0-PC, and diC18:0-PC were prepared by a reconstitution procedure that included the detergent but not MelB. Using fluorescence polarization with DPH as the probe, no significant difference in T_m values could be detected between vesicles prepared in the presence or the absence of detergent, thus indicating that the detergent was completely removed in all cases. On the other hand, the six to eight molecules of endogenous lipids copurified with MelB (see Materials and Methods) represent less than 2 mol % of the total lipids for MelB/phosphatidylcholine ratios of <1:400. We observed that mixing 2 mol % of purified endogenous lipids (mainly phosphatidylglycerol and phosphatidylethanolamine) to the various phosphatidylcholine species did not significantly alter their T_m values. Thus, the change in T_m can safely be related to the influence of the protein. For each lipid, the differences ΔT between the T_m measured in the presence and absence of protein were expressed in the form of the temperature versus protein composition diagrams shown in Figure 2. As can be seen, increasing the protein concentration progressively lowered the phase transition temperature of diC18:0-PC and to a lower extent of diC16:0-PC ($\Delta T < 0$) but increased that of diC14:0-PC and to a larger extent of diC12:0-PC ($\Delta T > 0$).

Influence of the Lipid Acyl Chains on Melibiose Permease Activity. Any attempt to strictly correlate MelB activity and
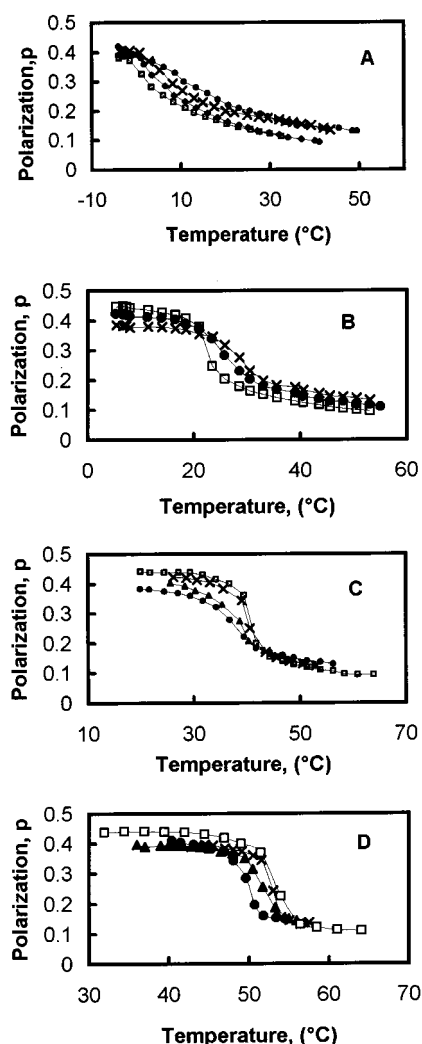
FIGURE 1: Polarization/temperature curves of DPH in proteoliposomes composed of melibiose permease reconstituted in various saturated phosphatidylcholine species. MelB permease was reconstituted in the four phosphatidylcholine species: (A) DiC12:0-PC, (B) DiC14:0-PC, (C) DiC16:0-PC, (D) DiC18:0-PC with various MelB/PC ratios. The polarization p of DPH was determined. The recombinants and molar ratios shown are as follows: (A) MelB/DiC12:0-PC 0 (□), 1:927 (◆), 1:400 (×), 1:217 (●); (B) MelB/DiC14:0-PC 0 (□), 1:882 (●), 1:212 (×); (C) MelB/DiC16:0-PC 0 (□), 1:300 (×), 1:258 (▲), 1:133 (●); (D) MelB/DiC18:0-PC 0 (□), 1:585 (×), 1:325 (▲), 1:131 (●).

FIGURE 2: Plot of ΔT versus protein-to-lipid ratio for MelB/phosphatidylcholine recombinants. The midpoint transition temperature of the various liposomes ($T_{m,0}$) and proteoliposomes (T_m) was determined. $\Delta T = (T_m - T_{m,0})$ was expressed as a function of X_p, the protein mole fraction in the lipids. The lipids used were DiC12:0-PC (◆), DiC14:0-PC (□), DiC16:0-PC (▲), and DiC18:0-PC (○).

FIGURE 3: Polarization/temperature curves of DPH in proteoliposomes composed of melibiose permease reconstituted in various unsaturated phosphatidylcholine species. DiC14:1-PC (*), DiC16:1-PC (△), DiC18:1-PC (○), and DiC20:1-PC (−).

bilayer thickness requires that all membrane phospholipids be in the same physical state. For that reason, diC12:0-PC and Δ9-cis monounsaturated PCs with 14, 16, 18, 20, and 22 carbon atoms in their acyl chains were used. With gel-to-liquid phase transition temperatures below 0 °C, these lipids were all in the liquid-crystalline phase at the temperature of 20 °C used for the transport activity measurements. MelB was incorporated at a protein-to-lipid ratio of 1/1000. It was important to check that the protein, even at this low concentration, did not significantly affect the physical state of the lipids. The various proteoliposomes were submitted to fluorescence polarization experiments, with DPH as the probe. Over the temperature range 20−45 °C, p exhibited relatively low values ($p < 0.3$) and slightly decreased with temperature (Figure 3), a behavior characteristic of lipids in the liquid-crystalline state. At given temperatures, the various proteoliposomes tested showed similar p values ($p = 0.27$
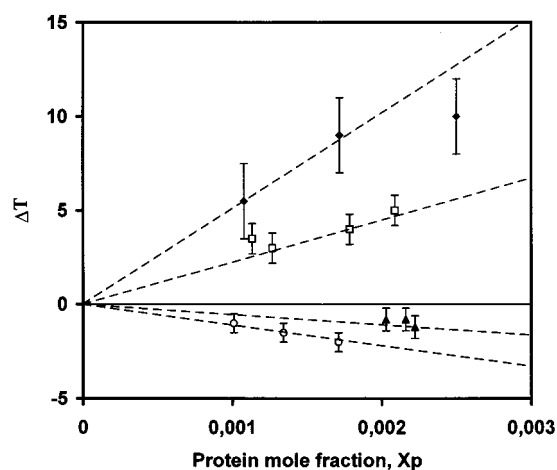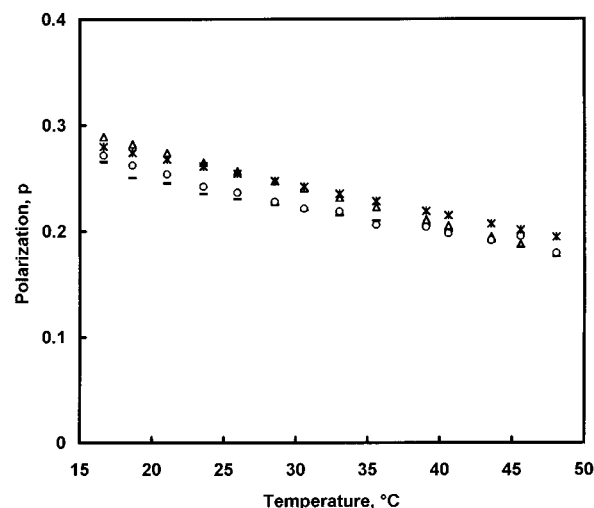
at 20 °C), which means similar dynamic states for the lipid acyl chains.

The influence of the lipids on the transport of melibiose by MelB was studied at two levels: (i) the binding capacity of the protein and (ii) its carrier activity.

Influence of the Lipid Acyl Chains on the Binding of Dansyl Galactoside. Sugar binding to MelB in reconstituted liposomes was studied by a fluorescence resonance energy transfer (FRET) method using the high-affinity galactoside analogue Dns[2]-S-Gal, whose fluorescence signal depends on the polarity of its environment (*52−54*). Typically, in proteoliposomes prepared from *E. coli* lipids and incubated with micromolar concentrations of the fluorescent sugar analogue, excitation of MelB tryptophans at 297 nm induces the emission of a fluorescence signal at 460 nm originating from Dns[2]-S-Gal bound to the sugar-binding site. A concomitant quenching of the Trp emission signal (340 nm) is observed. The signal which is recorded at 560 nm essentially
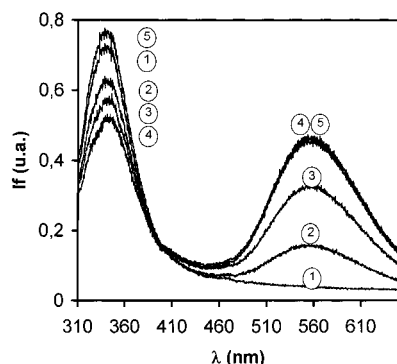
FIGURE 4: Effect of Dns^2-S-Gal on Trp and Dns^2-S-Gal fluorescence emission spectra. MelB permease was reconstituted in various phosphatidylcholine species at a protein-to-lipid ratio of 1/1000. Proteoliposomes were resuspended at 2.5 μg/mL in 100 mM KH$_2$PO$_4$, pH 7.0, 10 mM NaCl. Increasing concentration of Dns^2-S-Gal 0 (1), 2 μM (2), 5 μM (3), and 7.5 μM (4, 5) supplemented with 10 mM melibiose (5) were added. The excitation wavelength was 295 nm. The figure shows the data obtained with the MelB permease/DiC12:0-PC recombinant.

arises from free Dns^2-S-Gal in the medium. It increases with the analogue concentration. The changes in Dns^2-S-Gal (460 nm) and Trp (340 nm) signals are both Na$^+$-dependent and are completly reversed when melibiose is added in excess. Either signal can be used to titrate MelB sugar-binding activity. Figure 4 illustrates typical records (wavelength range 310– 570 nm) of the FRET signal from MelB proteoliposomes prepared with DiC12:0-PC. As reported for *E. coli* lipid/MelB proteoliposomes, Trp emission at 340 nm from PC/MelB proteoliposomes was quenched upon addition of Dns^2-S-Gal and restored when Dns^2-S-Gal bound to MelB was displaced by melibiose. Thus, the FRET transfer phenomenon occurred in PC/MelB proteoliposomes. In contrast, the specific Dns^2-S-Gal signal centered at 460 nm and typically recorded in *E. coli* lipid/MelB vesicles was no longer observed in PC/MelB vesicles (Figure 4). Also, no significant change in the 560-nm signal was observed when melibiose was added. Recalling that the fluorescence signal arising from Dns^2-S-Gal becomes weaker and is displaced toward higher wavelengths as its environment becomes more polar, the data suggest that the environment of the Dns^2-S-Gal molecules bound to MelB is more polar in PC- than in *E. coli*-proteoliposomes, implying in turn that MelB has a conformation that depends on the lipid polar heads and/or acyl chain composition. The former explanation seems more likely as similar FRET signals were recorded from vesicles containing PC species with different acyl chain lengths.

The affinity of Dns^2-S-Gal for MelB reconstituted in the various PC species was determined by measuring the quenching ΔF [$\Delta F = (F - F_0)$/mg of protein] of the Trp fluorescence signal resulting from addition of Dns^2-S-Gal. Figure 5 illustrates a typical experiment. With all PC species tested, the binding data suggested a single class of binding site with comparable binding constants ($K_d = 11 \pm 1$ μM and $B_{max} = 140 \pm 5$ au/mg of protein). It can be concluded that changing the acyl chain length did not perturb the binding of the sugar to MelB. Incidentally, one should note that the K_d values estimated from MelB reconstituted with phosphatidylcholines are 10-fold higher than those estimated in *E. coli* proteoliposomes (52), a finding that correlates with the loss of Dns^2-S-Gal signal (see above) and suggests an
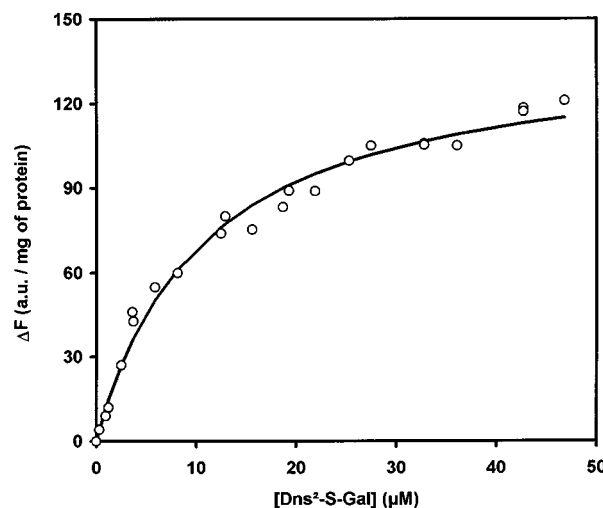

FIGURE 5: Binding of Dns^2-S-Gal on melibiose permease/ DiC12:0-PC proteoliposomes. The Trp fluorescence emission peak between 310 and 400 nm of the MelB proteoliposomes obtained in the presence of Dns^2-S-Gal (as described in Figure 4) were integrated. $\Delta F = (F_0 - F)$, in which F_0 and F are the fluorescence intensities obtained in absence and presence of Dns^2-S-Gal, respectively. For the sake of clarity, only the saturation curve obtained with MelB/DiC12:0-PC proteoliposomes is shown.
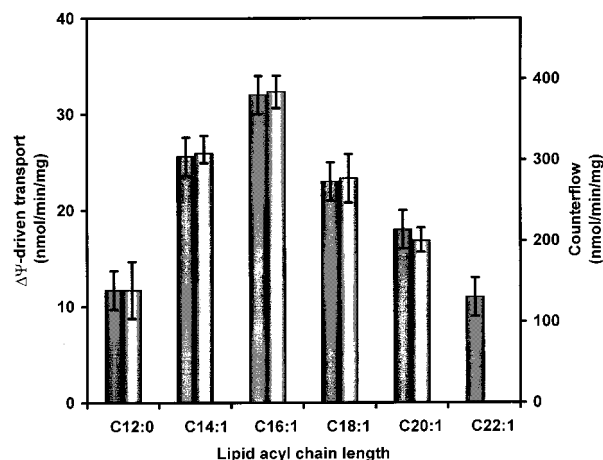

FIGURE 6: Influence of lipid acyl-chain length on $\Delta\psi$-driven melibiose transport and counterflow in proteoliposomes. The lipids were the saturated DiC12:0-PC and the unsaturated DiCn:1-PCs (from C14 to C22).

additional role of the lipid polar headgroups on MelB structure.

Influence of the Lipid Acyl Chains on Melibiose Uptake. In proteoliposomes containing purified MelB, [^{3}H]melibiose accumulation can be driven by an artificially imposed membrane potential ($\Delta\psi$, inside negative) generated by a valinomycin-induced potassium diffusion potential (36). With the various phosphatidylcholine species tested, the kinetics of the melibiose uptake were linear for at least 2 min. This melibiose accumulation depended on $\Delta\psi$ as it was completely abolished by addition of CCCP. A plot of the rate of melibiose uptake versus the lipid acyl chain lengths (Figure 6) showed a bell-shaped profile, the highest activity being supported by diC16:1-PC. Importantly, the transmembrane distribution of TPP in the various PC proteoliposomes indicated that $\Delta\psi$ was independent of the lipid composition (45 ± 5 mV). Thus, the observed differences in the $\Delta\psi$-driven melibiose uptake between the various PC proteoli-

posomes may be a direct consequence of the bilayer thickness.

The influence of the lipid acyl chain length on melibiose transport was studied with the counterflow technique as well. This technique enables the transport of melibiose to be studied in the absence of a $\Delta\psi$, thus providing another assessment of the carrier activity (*55*). All proteoliposome preparations exhibited a transient accumulation of melibiose caused by two competing processes, an exchange and an efflux reaction. Because the initial phase of counterflow represents the exchange activity of the carrier, the initial rate of melibiose uptake estimated from the amount of label accumulated during the first minute can be taken as a direct measurement of transporter activity. As can be seen in Figure 6, melibiose permease activities so determined were similar to those measured in the presence of a $\Delta\psi$, with the same bell-shaped dependence on lipid acyl chain length.

DISCUSSION

The aim of this study was to demonstrate that optimal functioning of a transmembrane protein requires good matching of its hydrophobic length with the hydrophobic thickness of the supporting lipid bilayer. Before discussing the influence of lipids on the activity of melibiose permease, it was important to demonstrate that the various MelB/lipid systems tested responded to the principle of hydrophobic matching. This was checked by investigating the influence of the protein on the physical state of the lipids.

Influence of MelB on the Physical State of the Lipids. The results presented above clearly indicated that MelB had a strong influence on the gel-fluid phase transition temperature of the various saturated PC species in which it was reconstituted. A rigidifying effect was observed with the short- and medium-chain length lipids diC12:0-PC and diC14:0-PC, while a fluidifying effect was detected with the long-chain molecules diC16:0-PC and diC18:0-PC. The shifts ΔT in transition temperature shown in Figure 3 were measured at low protein concentration in the lipids, a condition which permits them to be accounted for using the following relationship (*7, 56*):

$$\Delta T = 16\xi^2(\phi_p/\pi\xi + 1)[(d_m - d_p)/(d_{L,f} - d_{L,g})]X_p \quad (1)$$

In this equation, ξ is the characteristic coherence length of the lipid phase, ϕ_p is the perimeter of the protein, $d_m = 1/2(d_{L,f} + d_{L,g})$ is the mean hydrophobic thickness of the unperturbed lipid bilayer, d_p is the hydrophobic length of the protein, $d_{L,f}$ and $d_{L,g}$ are the hydrophobic thicknesses of the lipid bilayer in the fluid and gel phase, respectively, and X_p is the protein mole fraction. This equation is based upon elastic models within the Landau–de Gennes theory, which attributes the full excess free energy to an elastic distortion of the lipid phase. In the case of protein/lipid hydrophobic mismatch, the main elastic force results from an expansion or a compression of the lipid bilayer by the protein in the normal direction and changes in the hydrophobic thickness of the lipids in contact with the protein are derived from changes in the order parameter of their acyl chains (*7, 56*).

To be used, eq 1 requires the knowledge of structural parameters concerning both the lipids and the protein. $d_{L,f}$ and $d_{L,g}$ values used for the lipids are shown in Table 1. They were obtained as described in ref *4* and using the data

Table 1: Hydrophobic Lengths $d_{L,f}$ and $d_{L,g}$ of Hydrated Bilayers of DiCn:0-PCs and DiCn:1-PCs[a]

acyl chains	$d_{L,f} \pm 0.1$ nm	$d_{L,g} \pm 0.1$ nm	d_m
C12:0	1.95	2.7	2.3
C14:0	2.3	3.15	2.7
C16:0	2.6	3.6	3.1
C18:0	2.95	4.05	3.5
C14:1	2.3		
C16:1	2.65		
C18:1	3.0		
C20:1	3.35		

[a] Details on the way the values were obtained are given in ref *4*. Briefly, for the saturated species in the fluid phase, $d_{L,f}$ was obtained from the X-ray diffraction data of Lewis and Engelman (*59*) by removing 1.1 nm (2 × 0.55) to the phosphate to phosphate transbilayer distance. In the gel state, $d_{L,g}$ was obtained from the X-ray diffraction data published for diC14:0-PC (*57, 58*) and diC16:0-PC (*58*) still by removing 1.1 nm to the phosphate to phosphate transbilayer distance. For the four lipids, $d_{L,g}$ was also determined through direct calculation assuming elongated acyl chains oriented at 30° with respect to the bilayer normal. Consistently, the $d_{L,g}$ values so obtained may be deduced from the corresponding $d_{L,f}$ values as $d_{L,g} \approx 1.37 d_{L,f}$. d_m is the mean hydrophobic thickness ($d_{L,f} + d_{L,g}$)/2. For the unsaturated species, $d_{L,f}$ was deduced from X-ray (*59, 60*) and molecular dynamics simulations (*61*) data as above. $d_{L,f}$ values relate to lipids with nearly constant molecular area of 0.66 nm^2 for the saturated species and 0.68 nm^2 − 0.70 nm^2 for the unsaturated ones.

Table 2: Prediction of the Length of the Transmembrane Segments of MelB Permease[a]

helix	I	II	III	IV	V	VI	VII	VIII	IX	X	XI	XII
no. of residues	20	17	21	23	18	21	26	20	18	19	19	20
hydrophobic length mean							3.02 nm					

[a] The amino acid sequence of MelB was submitted to the predict protein server available for fully automatic use by electronic mail to the Internet address (PredictProtein@EMBL-Heidelberg-de). The sequences of the various α helices are given by the server and allowed us the prediction of their hydrophobic length expressed in number of amino acid residues

in ref *57−61*. With respect to the protein, structural data are lacking. However, according to the statistical analysis of packing preferences of transmembrane proteins published by Bowie (*62*), the 12 α-helices of MelB may be assumed to pack within the membrane, via helix−helix interactions. The area covered by one α-helix may be estimated at 1 nm^2 from the crystallographic structure of bacteriorhodopsin, a bundle of seven closely packed α-helices with a cross sectional area of ∼7 nm^2 (*63, 64*). For a bundle of 12 α-helices and assuming a circular cross-section, this means a minimum area of 12 nm^2 to which corresponds a perimeter ϕ_p of 12.3 nm. From hydropathy prediction methods and various topographic studies (*39*), a mean length of about 20 amino acids was estimated for the 12 hydrophobic membrane-spanning segments of the protein. In the present work, this length was also estimated using a powerful neural prediction method (Predict Protein) available via Internet to the EMBL site (PredictProtein@EMBL-Heidelberg-de). To strengthen the prediction, five MelB primary sequences from different origins were compared. Results concerning that for *E. coli* are shown in Table 2. Eight out of the 12 hydrophobic helices ranged between 19 and 23 amino acid residues while three were shorter and one was longer, with a mean length of 20 amino acids. Normally, the mean hydrophobic length d_p of the protein should be estimated by considering only the

helical segments which are in contact with the lipids and by taking into account their orientation with respect to the bilayer normal. In the absence of any precise data on the topology and conformation of MelB in the membrane, the d_P value of 3.02 nm given in Table 2 was calculated by averaging over the 12 α-helices considered oriented parallel to the bilayer normal. Finally, the coherence length ξ is a physical parameter which characterizes the lipid bilayer and which may slightly vary depending on the lipid and protein molecules in the presence. A value of 1.5 nm was proposed by Jähnig on a theoretical basis (*65*). It was conveniently used by Peschke et al. (*7*) to account for the data obtained with the reaction center protein recombined with ditride-canoylphosphocholine. In the case of bacteriorhodopsin in diC12:0-PC, best fitting of the data was achieved with a slightly lower ξ value of 1.0 nm (*21*).

For each lipid, in agreement with the theory and within experimental error, the midpoint transition temperature, T_m, shifted linearly with increasing MelB concentration and these shifts in T_m (ΔT in Figure 3) were closely related to the lipid/protein hydrophobic mismatch ($d_m - d_P$), both in sign and amplitude. The theory also predicts that $\Delta T = 0$ for $d_p = d_m$, which suggests a hydrophobic length for the protein slightly smaller than the mean hydrophobic thickness of diC16:0-PC, i.e., 3.1 nm.

In principle, since the conformation and, therefore, the size of the protein may depend on the extent of the hydrophobic mismatch, eq 1 should be used with ϕ_p and d_p values appropriate to each lipid. However, making the reasonable approximation that conformational changes of MelB are of small amplitude and without noticeable consequence on its size and also that ξ remains unchanged for the set of lipids tested, d_P may be estimated using eq 2, which derives from the comparison of the ΔT values obtained for two lipids L1 and L2 and in which now d_p is the sole unknown parameter:

$$(\Delta T_{L1}/X_{p,L1})/(\Delta T_{L2}/X_{p,L2}) = [(d_{m,L1} - d_P)/(d_{m,L2} - d_P)][(d_{L2,f} - d_{L2,g})/(d_{L1,f} - d_{L1,g})] \quad (2)$$

Consistently, systematic comparison of the lipids two by two and for the varying protein mole fraction tested led to a set of 80 dp values centered around 3.0 ± 0.1 nm. Interestingly, the d_p value of 3.0 nm measured in this way, is similar to the 3.02 nm estimated from hydropathy profiles. In addition to the fact that ΔT varied linearly with X_P, these results indicate an absence of protein aggregation in the lipids, at least over the concentration range $X_P < 1/400$ of interest. Using this d_p value of 3 nm, it was possible to reevaluate ϕ_p using eq 1 and with given ξ values. If the theoretical value of 1.5 nm was used, best fitting of eq 1 to the data in Figure 3 was achieved with ϕ_p of ∼8 nm, a perimeter much smaller than the 12.3 nm estimated for a bundle of 12 α-helices. Actually, and in good agreement with the bacteriorhodopsin/diC12:0-PC system (ξ ≈ 1.0 nm) (*21*), a perimeter of 12.3 nm was accounted for with ξ ≈ 1 nm.

From these observations, one can conclude that the MelB/diCn:0-PC proteoliposomes responded to the hydrophobic matching principle. The protein showed substantial influence on the physical state of the lipids which can be accounted for by the theory. Consistent with the d_P value estimated from sequence analysis, an important conclusion is that the

hydrophobic matching condition, when sensed by the lipids, is satisfied for a lipid bilayer whose mean hydrophobic thickness is around 3 nm. May this condition have functional consequences?

Influence of the Bilayer Thickness on MelB Activity. Correlation between Hydrophobic Mismatch and Transport Activity. Melibiose transport implies the binding and then the transport of the sugar. Spectroscopic analysis of the interaction of the fluorescent sugar analogue with MelB indicates that sugar binding to the transporter does not strongly depend on the acyl chain composition of the surrounding lipids. In contrast, the rate of counterflow or of $\Delta\psi$-driven melibiose transport both depend on the lipid acyl chain length, with a similar bell-shaped profile. It is important to recall that the two transfer reactions involve a common partial step, namely the coupled influx of Na ions and sugar, and that this translocation step is known to be rate limiting for each reaction (*55*). Taken together, these findings suggest that the influx reaction is dependent on the acyl chain composition of the lipids surrounding the MelB.

It has been suggested that changes in protein activity may be related to changes in membrane fluidity (*66–69*). In agreement with another proposition (*70*), the fact that in our experiment**s** the physical state of the lipids was not affected by the length of their acyl chains means that such an explanation may be discarded. Instead, protein/lipid hydrophobic mismatch, which has been demonstrated above to operate at the lipid level, is more than likely responsible for the observed changes in transport activity. Optimum activity was found in diC16:1-PC, a lipid whose hydrophobic thickness in the liquid state is 2.65 nm (Table 1), smaller than the 3 nm estimated for the protein d_P. At first sight, optimum activity might have been expected to be found in diC18:1-PC whose hydrophobic thickness of 3.0 nm in the liquid state matches that of the protein. Actually, due to various local constraints of free volume reduction (*71*) and compression−expansion (*72–74*), acyl chains in contact with the protein are expected to elongate, explaining why best matching and, therefore, activity were found in diC16:1-PC and not in diC18:1-PC. From all these results, it may be concluded that the transport of melibiose by MelB is modulated by the acyl chain length of the surrounding lipids in response to a hydrophobic mismatch, maximum transport activity being reached when the protein/lipid hydrophobic matching condition is optimum.

The $\Delta\psi$-driven and counterflow processes share the inward/outward translocation step of the sugar across the membrane, via a ternary Na/melibiose/MelB complex (*48, 55*). The similarity in transport rate profiles and the absence of influence of lipids on K_D strongly suggest this translocation step is rate limiting and is directly influenced by the lipid environment. If the influence of the protein on the lipids may be interpreted in a straightforward manner in terms of acyl chain flexibility and order, the consequences of hydrophobic mismatch on protein activity are more difficult to analyze.

Compression−expansion of the acyl chains (*72–74*), and more subtle effects such as splay-distortion, surface tension (*73*), and line tension of the lipids in contact with the protein (*74*), may independently or in combination trigger an aggregation of the proteins or changes in their conformation (*72*). With MelB, transport experiments were carried out with a protein-to-lipid ratio of 1/1000, well below that of 1/400

up to which the protein was shown, in the above section, to stay in the monomeric form in the lipid bilayers. For large polytopic proteins, and in particular for those endowed with carrier activity, conformational changes may be thought as first of corresponding to modifications in the relative orientation of the transmembrane segments. Accordingly, an increase in the concentration of lactose permease (a 12 α-helices transmembrane protein from *E. coli*) in lipids has recently been shown to result in a continuous decrease in transport activity in a manner that correlates with an increase in the average tilt angle of the helices with respect to the bilayer normal (*75*). In the same respect, the orientation with respect to the bilayer normal of a synthetic α-helical peptide of 19 amino acids was shown to depend on the lipid acyl chain length and to be optimal for 18−20 carbon atoms (*76*). Changes in the orientation of the transmembrane segments of MelB in response to a hydrophobic mismatch could explain the observed changes in transport activity.

In conclusion, we have shown that the melibiose permease activity is controlled by the extent of protein/lipid hydrophobic mismatch. If the acyl chain length of the lipids surrounding MelB does not match the transporter membrane domain, its activity is strongly impaired. These results suggest that the protein/lipid hydrophobic mismatch plays a considerable role by inducing conformational changes, which affect not only the lipids but certainly also the proteins. Although not investigated in detail, several findings in the present paper also point toward an important role for the lipid headgroups on MelB structure and/or function. At the level of biological membranes, we think that a mechanism of molecular sorting may operate to satisfy this potential specificity between the protein and the headgroups and/or the acyl chains of the lipids (*4*). Cross influence of lipid acyl chains and polar headgroups on MelB activity is currently under investigation in our laboratory.

ACKNOWLEDGMENT

REFERENCES

1. Mouritsen, O. G., and Bloom, M. (1984) *Biophys. J. 46*, 141−153.
2. Mouritsen, O. G., and Bloom, M. (1993) *Annu. Rev. Biophys. Biomol. Struct. 22*, 145−171.
3. Killian, A. (1998) *Biochim. Biophys. Acta 1376*, 401−416.
4. Dumas, F., Lebrun, M. C., and Tocanne, J. F. (1999) *FEBS Lett. 458*, 271−277.
5. Sperotto, M. M., and Mouritsen, O. G. (1991) *Eur. Biophys. J. 19*, 157−68.
6. Sperotto, M. M., and Mouritsen, O. G. (1993) *Eur. Biophys. J. 22*, 323−328.
7. Peschke, J., Riegler, J., and Möhwald H. (1987) *Eur. Biophys. J. 14*, 385−391.
8. Ryba, N. J. P., and Marsh, D. (1992) *Biochemistry 31*, 7511−7518.
9. Cornea, R. L., and Thomas, D. D. (1994) *Biochemistry 33*, 2912−2920.
10. Dumas, F., Sperotto, M. M., Lebrun, M. C., Tocanne, J. F., and Mouritsen O. G. (1997) *Biophys. J. 73*, 1940−1953.
11. Horowitz, A. D. (1995) *Chem. Phys. Lipids 76*, 27−39.
12. Lehtonen, J. Y., and Kinnunen, P. K. (1997) *Biophys. J. 72*, 1247−1257.
13. Bretscher, M. S., and Munro S. (1993) *Science 261*, 1280−1281.
14. Munro, S. (1995) *Biochem. Soc. Trans.23*, 527−530.
15. Masibay, A. S., Balaji, P. V., Boeggeman, E. E., and Qasba, P. K. (1993) *J. Biol. Chem. 268*, 9908−9916.
16. Webb, R. J., East, J. M., Sharma, R. P., and Lee, A. G. (1998) *Biochemistry 37*, 673−679.
17. Nezil, F. A., and Bloom, M. (1992) *Biophys. J. 61*, 1176−1183.
18. Riegler, J., and Mohwald H. (1986) *Biophys. J. 49*, 1111−1118.
19. Kurrle, A., Rieber, P., and Sackmann, E. (1990) *Biochemistry 29*, 8274−8282.
20. Zhang Y. P., Lewis, R. N., Hodges, R. S., and MacElhaney (1992) *Biochemistry 31*, 11572−11578.
21. Piknova, B., Perochon, E., and Tocanne, J. F. (1993) *Eur. J. Biochem. 218*, 385−396.
22. Froud, R. J., Earl, C. R. A., East, J. M., and Lee, A. G. (1986) *Biochim. Biophys. Acta 860*, 354−360.
23. Caffrey, M., and Feigenson G. W. (1981) *Biochemistry 20*, 1949−1961.
24. Johannsson, A., Keightley, C. A., Smith, G. A., Richards, C. D., Hesketh, T. R., and Metcalfe, J. C. (1981) *J. Biol. Chem. 256*, 1643−1650.
25. Starling, A. P., East, J. M., and Lee, A. G. (1993) *Biochemistry 32*, 1593−1600.
26. Lee, A. G. (1998) *Biochim. Biophys. Acta 1376*, 381−390.
27. Johannsson, A., Smith, G. A., and Metcalfe, J. C. (1981) *Biochim. Biophys. Acta 641*, 416−421.
28. Carruthers, A., and Melchior D. L. (1984) *Biochemistry 23*, 6901−6911.
29. In't Veld, G., Driessen, A. J. M., Op den Kamp, J. A. F., and Konings, W. N. (1991) *Biochim. Biophys. Acta 1065*, 203−212.
30. Uratani, Y., Wakayama, N., and Hoshino, T. (1987) *J. Biol. Chem. 262*, 16914−16919.
31. Montecucco, C., Smith, G. A., Dabbeni-Sala, F., Johannsson, A., Galante, Y. M., and Bisson, R. (1982) *FEBS Lett. 44*, 145−148.
32. Pourcher, T., Sarkar, H. K., Bassilana, M., Kaback, H. R., and Leblanc, G.(1990) *Proc. Natl. Acad. Sci. U.S.A. 87*, 468−472.
33. Wilson, D. M., and Wilson, T. H. (1992) *J. Bacteriol. 174*, 3083−3086.
34. Reizer, J., Reizer, A., and Saier, M. H., Jr. (1994) *Biochim. Biophys. Acta 1197*, 133−166.
35. Yazyu, H. S., Shiota-Niiya, S., Shimamoto, T., Kanazawa, H., Futai, M., and Tsuchiya, T. (1984) *J. Biol. Chem. 259*, 4230−4236.
36. Pourcher, T., Leclercq, S., Brandolin, G., and Leblanc, G. (1995) *Biochemistry 34*, 4412−4420.
37. Botfield, M. C., Naguchi, K., Tsuchiya, T., and Wilson T. H. (1992) *J. Biol. Chem. 267*, 1818−1822.
38. Gwizdek, C., Leblanc, G., and Bassilana, M. (1997) *Biochemistry 36*, 8522−8529.
39. Pourcher, T., Bibi, E., Kaback, H. R., and Leblanc, G. (1996) *Biochemistry 35*, 4161−4168.
40. Pourcher, T., Deckert, M., Bassilana, M., and Leblanc, G. (1991) *Biochem. Biophys. Res. Commun. 178*, 1176−1181.
41. Botfield, M. C., and Wilson T. H. (1988) *J. Biol. Chem. 263*, 12909−12915.
42. Mus-Veteau, I., and Leblanc, G. (1996) *Biochemistry 35*, 12053−12060.
43. Rigaud, J. L., Paternostre, M. T., and Bluzat, A. (1988) *Biochemistry 27*, 2677−2688.
44. Richard, P., Rigaud, J. L., and Graber P. (1990) *Eur. J. Biochem. 193*, 921−925.
45. Rigaud, J. L., Pitard, B., and Levy, D. (1995) *Biochim. Biophys. Acta 1231*, 223−246.
46. Paternostre, M. T., Roux, M., and Rigaud, J. L. (1988) *Biochemistry 27*, 2668−2677.
47. Heyn, M. P., and Dencher, N. A. (1982) *Methods Enzymol. 88*, 31−35.
48. Bassilana, M., Pourcher T., and Leblanc G. (1987) *J. Biol. Chem. 262*, 16865−16870.

49. Oku, N., Kendall, D. A., and MacDonald, R. C. (1982) *Biochim. Biophys. Acta 691*, 332−340.

50. Lowry, O. H., Rosebrough, N. J., Farr, A. L., and Randall, R. J. (1951) *J. Biol. Chem. 193*, 265−275.

51. Eaton, B. R., and Dennis, E. A. (1976) *Arch. Biochem. Biophys. 176*, 604−609.

52. Maehrel, C., Cordat, E., Mus-Veteau, I., and Leblanc, G. (1998) *J. Biol. Chem. 273*, 33192−33197.

53. Reeves, J. P., Shechter, E., Weil, R., and Kaback, H. R. (1973) *Proc. Natl. Acad. U.S.A. 70*, 2722−2726.

54. Schuldiner, S., Kerwar, G. K., Kaback, H. R., and Weil, R. (1975) *J. Biol. Chem. 250*, 1361−1370.

55. Bassilana, M., Pourcher, T., and Leblanc G. (1988) *J. Biol. Chem. 263*, 9663−9667.

56. Sperotto, M. M., and Mouritsen, O. G. (1988) *Eur. Biophys. J.16*, 1−10.

57. Janiak, M. J., Small, D. M., and Shipley, G. G. (1979) *J. Biol. Chem. 254*, 6068−6078.

58. Janiak, M. J., Small, D. M., and Shipley, G. G. (1976) *Biochemistry 15*, 4575−4580.

59. Lewis, B. A., and Engelman, D. M. (1983) *J. Mol. Biol. 166*, 211−217.

60. Wiener, M. C., and White, S. H. (1992) *Biophys. J. 61*, 434−447.

61. Feller, S. E., Yin, D., Pastor, R. W., and MacKerell, A. D. (1997) *Biophys. J. 73*, 2269−2279.

62. Bowie, J. U. (1997) *J. Mol. Biol. 272*, 780−789.

63. Henderson, R., and Unwin, P. N. (1975) *Nature 257*, 28−32.

64. Henderson, R., Baldwin, J. M., Ceska, T. A., Zemlin, F., Beckmann, E., and Downing, K. H. (1990) *J. Mol. Biol. 213*, 899−929.

65. Jähnig, F. (1981) *Biophys. J. 36*, 329−345.

66. Thilo, L., Trauble, H., and Overath, P. (1977) *Biochemistry 16*, 1283−1290.

67. Silvius, J. R., and McElhaney, R. N. (1980) *Proc. Natl. Acad. Sci. U.S.A. 77*, 1255−1259.

68. Dufour, J. P., and Tsong, T. Y. (1981) *J. Biol. Chem. 256*, 1801−1808.

69. Moore, B. M., Lentz, B. R., Hoechli, M., and Meissner, G. (1981) *Biochemistry 20*, 6810−6817

70. Lee, A. G. (1991) *Prog. Lipid Res. 30*, 323−348.

71. Almeida, P. F. F., Vaz, W. L. C., and Thompson, T. E. (1992) *Biochemistry 31*, 7198−7210.

72. Gil, T., Ipsen, J. H., Mouritsen, O. G., Sabra, M. C., Sperotto, M. M., and Zuckermann, M. (1998) *Biochim. Biophys. Acta 1376*, 245−266.

73. Nielsen, C., Goulian, M., and Andersen, O. S. (1998) *Biophys. J. 74*, 1966−1983.

74. Dan, N., and Safran, S. A. (1998) *Biophys. J. 75*, 1410−1414.

75. Le Coutre, J., Narasimhan, L. R., Kumar, C., Patel, N., and Kaback, H. R. (1997) *Proc. Natl. Acad. Sci. U.S.A. 94*, 10167−10171.

76. Ren, J., Lew, S., Wang, Z., and London, E. (1997) *Biochemistry 36*, 10213−10220.